# Controlling the magnetic anisotropy in epitaxial Cr₂O₃ clusters by an electric field

David Halley,[*] Nabil Najjari, Florian Godel, Mohamad Hamieh, Bernard Doudin, and Yves Henry

*Institut de Physique et Chimie des Matériaux de Strasbourg, CNRS/UDS, 23 Rue du Loess, Boîte Postale 43,*
*F-67034 Strasbourg, Cedex 2, France*

Magnetic properties of $Cr_2O_3$ epitaxial clusters inserted in an Fe/MgO/Fe tunnel barrier are revealed by their tunnel magnetoresistance signature. The cluster assembly has been shown in a previous work to behave as a superparamagnet when a magnetic field was applied in the plane of the tunnel junction. We here demonstrate that an external large out-of plane electric field (in the order of 0.5 GV/m) favors in-plane magnetization orientation. This is due to an electric-field-induced magnetic anisotropy along the normal to the plane, corresponding to large anisotropy fields reaching up to 2 T. The assembly of clusters is thus strictly speaking not superparamagnetic and its magnetization cannot be exactly described by a Langevin law. This is attributed either to a strain-induced enhanced magnetoelectric effect or to a voltage-induced change of the magnetic anisotropy at interfaces with MgO.

## I. INTRODUCTION

Magnetoelectric materials, in which the magnetization can be driven by an electric field, are extensively studied for technological applications as memories or spintronic devices. Manipulating the magnetization of magnetic memories with an applied voltage would, for instance, open the way to a new generation of devices, with a high speed and low-power writing of information bits. Magnetoelectric materials have been experimentally studied for 50 years, since the observation of this effect in $Cr_2O_3$ [1–3], but there is still a lack of good candidates for technological applications: the magnetoelectric coefficient is too low in single-phase materials to allow the manipulation of magnetization under voltages achievable in devices.

Some theoretical predictions have suggested that the stress in epitaxial thin films can modify the magnetoelectric coefficient values, giving the opportunity to enhance this effect [4]. Moreover, different calculations based on Landau models [5–7] underlined the size and stress effects in magnetoelectric nanoparticles. The stress in such particles was predicted to possibly dramatically enhance the magnetoelectric coefficients and lead in some cases to the appearance of a multiferroic phase—for instance, ferromagnetic or ferroelectric—that is not observed in the bulk. Generally speaking, the low dimensionality of systems may favor the appearance of magnetoelectric effects, due for instance to symmetry breaking at interfaces [8].

We recently gave an experimental confirmation [9] of those predictions: $Cr_2O_3$, in the form of highly stressed epitaxial clusters, exhibits a permanent magnetization—whereas it is an antiferromagnet in its bulk phase—and huge magnetoelectric coefficients, three orders of magnitude larger than in the bulk. These observations were obtained on $Cr_2O_3$ clusters inserted in the MgO barrier of Fe/MgO/Fe magnetic tunnel junctions [Fig. 1(a)]: the voltage bias imposed an electric field on the tunnel barrier, while the magnetic properties of these nanoparticles were measured through their tunnel magnetoresistance (TMR) signature, with a magnetic field

applied in the plane of the junction. The $R(H)$ curves corresponded to a two-step tunneling of electrons via the $Cr_2O_3$ clusters; a Langevin curve fitting suggested that the cluster assembly was superparamagnetic and temperature-dependent measurements as a function of $H/T$ confirmed this behavior. The average modulus of the magnetic dipole $m$ of a cluster at a given electric field was then extracted from those fits; we observed a dramatic non-linear decrease of $m$ with the voltage value, irrespective of the voltage polarity.

We here further study the influence of an electric field on these clusters' magnetization, and more precisely we question the possibility of an electric-field-induced magnetic anisotropy. As we already claimed, the Langevin shape of the $R(H)$ curves was interpreted in our previous measurements as an indication of a superparamagnetic state for the cluster assembly, without any noticeable magnetic anisotropy. Nevertheless, a quite common feature in magnetoelectric materials is a change of magnetic anisotropy under an electric field [10]. This effect was for instance observed specifically at the interface of different magnetic metals with insulating layers: the most striking example can be found in FePt and FePd alloys [11] or in Fe/MgO systems [12,13], where the magnetic anisotropy can be dramatically modified through the voltage bias applied to the junction.

Our recent work on $Cr_2O_3$ nanoparticles [9] did not give us access to this anisotropy value due to the chosen geometry: TMR measurements are sensitive only to the projection of the magnetization of the clusters on the Fe electrode magnetization, which are in the plane of the junctions [Fig. 1(a)]. If a magnetic anisotropy axis were present in our system, perpendicular to the plane of the junction, it would not break the axial symmetry of the cluster magnetization around **n**, the normal to the plane. The calculation of the in-plane component of the magnetization, $M_{||}$, is in this case not analytically tractable [14] but numerical calculations—see Ref. [14] and our calculations reported below—show that the $M_{||}(H)$ curves are in this case very close to Langevin curves. Our previous observations thus could not discriminate between isotropic and anisotropic distribution of the cluster magnetization.

In order to address this question, we here report an added set of TMR measurements performed on the same stack as

————
[*]david.halley@unistra.fr
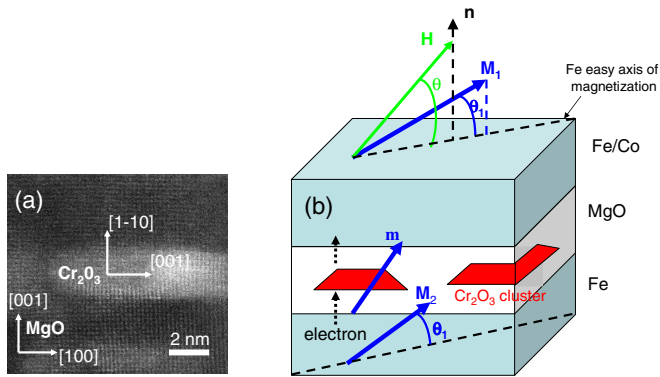
FIG. 1. (Color online) (a) Transmission electron microscopy image in cross section of a $Cr_2O_3$ cluster. (b) Schematic figure of the magnetic tunnel junctions with $Cr_2O_3$ clusters inserted inside the MgO barrier. The magnetic field makes an angle $\theta$ relative to the plane and forces the Fe electrodes' magnetization $M_1$ and $M_2$ to make an angle $\theta_1$ relative to the plane. The electric field is applied along **n**.

described above, but with an angle $\theta$ between the magnetic field **H** and the plane of the films [15]. When the possible anisotropic axis **n**, normal to the plane, is not perpendicular to the applied field, $M_{//}$ is not expected to follow a Langevin law. We experimentally show that an almost isotropic distribution of cluster magnetization is still observed under low voltages but is not found at higher voltages, in the order of 0.5 V. This reveals the occurrence of an electric-field-induced magnetic anisotropy that favors a magnetization direction perpendicular to the applied electric field.

## II. EPITAXIAL GROWTH OF THE DEVICES

Modified Co/Fe/MgO/Fe(001) magnetic tunnel junction stacks [16,17] on a MgO(100) susbtrate were fabricated by molecular beam epitaxy as detailed in Ref. [9]. We interrupted the growth of the 5.5 nm-thick MgO insulating layer after 2.5 nm to allow the deposition of a 0.3 nm chromium layer at 200 °C. This epitaxial growth of chromium on a smooth MgO(001) surface [18] resulted in the formation of nanometric flat clusters. Total oxidation of the clusters embedded in MgO was obtained by annealing the stack after growth completion [9,16,19]. For a nominal chromium thickness $t_{Cr} = 0.3$ nm, the resulting particles are typically 2 nm thick and 6 nm wide [see Fig. 1(a)]. X-ray absorption spectroscopy and transmission electron microscopy measurements [9] indicated that, under these conditions, the chromium particles fully oxidize into $Cr_2O_3$, which has a corundum structure. The corundum $c$ axis is along the in-plane [100] or [010] direction of MgO [Fig. 1(a)] and this structure is epitaxial on MgO(100) with a large compressive strain in the percent range. A small contribution of $Cr^{4+}$ ions to the magnetization of the clusters was also observed by x-ray circular magnetic dichroism in Ref. [9], but it involves less than 7% of the chromium ions and less than 20% of the magnetization of the clusters.

Tunnel junctions in the tens of microns diameter range were defined on those stacks by photolithography, $SiO_x$ deposition, and $Ar^+$ etching, as in Refs. [9] and [16]. The very low magnetization of the clusters combined with the requirement

of fabricating micrometric tunnel junctions means that the magnetic signal cannot be assessed by classical magnetometry techniques, which moreover are not compatible with the application of a very high electric field to the tunnel barrier.

## III. OUT-OF-PLANE MAGNETOTRANSPORT MEASUREMENTS

### A. Presence of magnetic anisotropy in $Cr_2O_3$ clusters

The devices can be regarded as double magnetic tunnel junctions, where electrons, finding available states in $Cr_2O_3$ clusters can tunnel from one Fe electrode to a cluster and from this cluster to the other electrode. Figure 2 gives an example of a typical TMR($H$) curve, obtained at $\theta = 0$; the superparamagnetic behavior of the embedded clusters leads to a continuous decrease of the resistance as the clusters' assembly magnetization aligns along the applied magnetic field. At low field, in-between the electrode coercive fields $H_{c1}$ and $H_{c2}$, the magnetization directions of the two electrodes are antiparallel, and the slope of the TMR($H$) curve is modified relatively to the rest of the curve [9] where the two electrodes have their magnetizations parallel. As shown in Ref. [9] the curves obtained at $\theta = 0$ can be fitted by Langevin curves (see Fig. 3), from which we extract an individual average magnetic dipole $m$ for the clusters, at different voltages. Indeed, the total resistance of a junction can be written $R = R_1 + R_2 + (\Delta R_1 + \Delta R_2) \cdot \mathcal{L}(\mu_0 m H / k_B T)$ in a sequential tunneling model, where $R_1$ and $R_2$ are constant resistances and $\Delta R_1$ and $\Delta R_2$ are spin-dependent resistances associated with the tunneling between, respectively, the bottom electrode and the cluster and the cluster and the top electrode and $\mathcal{L}$ is the Langevin function [20].

As shown in Ref. [9], this fitting of the TMR($H$) curves remains correct to the first order in the case of a cotunneling mechanism through the clusters. Moreover, this formula is quite general, and does not suppose any hypothesis concerning
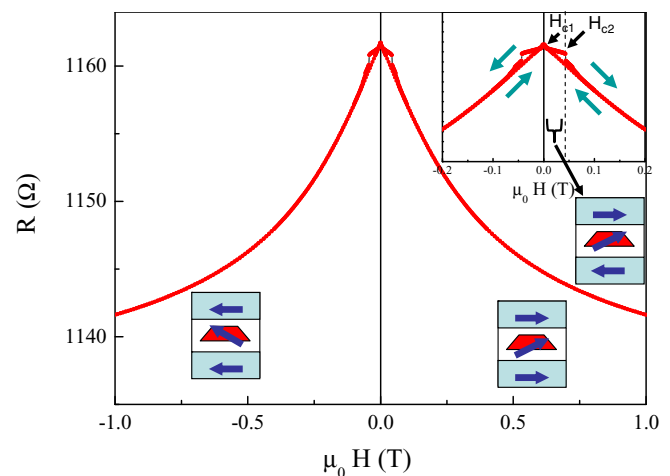


FIG. 2. (Color online) TMR($H$) measurement performed at 6.2 K under a −400 mV bias voltage at $\theta = 0$, showing a complete loop with increasing and decreasing magnetic field. The relative orientation of the electrodes and cluster magnetization is given as a sketch. Inset: zoom on the low-magnetic-field range, between the coercive fields $H_{c1}$ and $H_{c2}$ of the two electrodes. The magnetic field sweep direction is indicated.
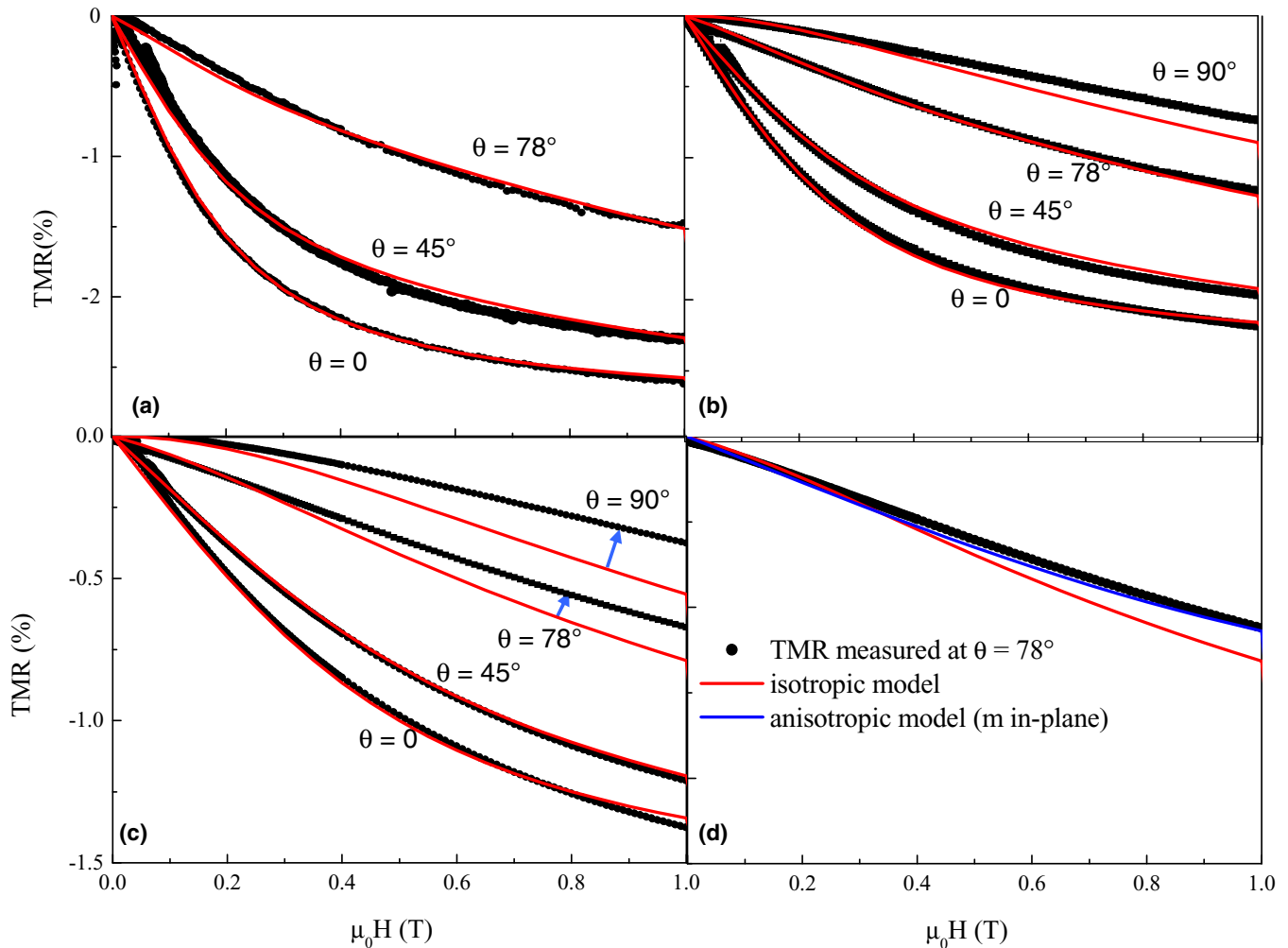
FIG. 3. (Color online) Angle-dependent TMR measurements. Measured TMR($H$) curves at different $\theta$ angle values (black dots) and TMR($H$) curves calculated within an isotropic model at different voltages $V$ (lines). (a) $V = -50$ mV. (b) $V = -200$ mV. (c) $V = -600$ mV. (d) The experimental TMR($H$) curve, at $\theta = 78°$ for $V = -600$ mV, and comparison with the isotropic model (red line) and a model supposing an in-plane confined magnetisation with the same $m$ value (blue line).

the nature of the tunneling electrons: the likely symmetry filtering [21] in our epitaxial stacks may influence the spin polarization of the tunneling electrons (and thus the $\Delta R_1$ and $\Delta R_2$ values) but not the dependence on the average direction of the cluster magnetization, which is given by the Langevin law.

Angle-dependent TMR measurements are performed at 6.2 K with a magnetic field **H** making a variable angle $\theta$ relative to the plane [Fig. 1(b)]. The projection of **H** in the film plane $H_{\parallel}$ is along Fe[100], i.e., along the easy axis of the Fe and Fe/Co electrodes. Measurements performed at $\theta \neq 0$ (Fig. 3), also show continuous TMR($H$) curves, whose shape and amplitude are modified as $\theta$ increases. If we suppose that the oxidized chromium clusters are superparamagnetic, then without any magnetic anisotropy, their magnetic moment resultant is along **H** whatever is $\theta$, and its modulus follows a Langevin law. On the other hand, the magnetoresistance value relates to the magnetic moment resultant projection along **M**$_1$ and **M**$_2$, which, in our geometry, are no longer parallel to **H**, except at $\theta = 0$. A calculation of the average angle between the cluster and electrode magnetizations is given in the Appendix, under this hypothesis. This calculation takes into account the

effect of the perpendicular component of **H**: the electrode magnetizations are no longer in plane but make an angle $\theta_0$ relative to the plane.

Figure 3 shows the TMR($H$) curves calculated from the isotropic model, for several different values of $\theta$ between 0 and 90°. No parameters or normalizations are used in this model: we use only the $m$ value obtained from the fit at the same bias voltage $V$ at $\theta = 0$ to calculate the expected curves at $\theta \neq 0$. We can see that, at low voltage values ($V = -50$ mV), the calculated curves are in quite good agreement with the experimental data obtained at different angles. This is not the case at larger bias voltage, with a discrepancy more pronounced when $\theta$ is increased: for instance, the curve obtained through the model at 78° fits well the experimental data at $V = -50$ mV, but the difference from the experimental data is large at $-600$ mV. The hypothesis of isotropic super-paramagnetic clusters cannot account for the TMR properties at high bias, whereas it holds at low voltage. We can therefore infer that the electric field across the clusters implies a magnetic anisotropy. Figure 3(d) illustrates this hypothesis by showing the TMR($H$) curve calculated under

the assumption of cluster magnetization confined in plane, i.e., if **n** were a strong magnetic hard axis. This simulation, though not perfect, better fits the experimental data measured at $\theta = 78°$ under a $-600$ mV voltage. This curve was calculated, as described in the Appendix, supposing an anisotropy field of 10 T forcing the cluster magnetization in plane, and assuming the same $m$ value as in the isotropic model.

We can infer from this observation that higher electrical fields favor an in-plane magnetization. We detail below the magnetic anisotropy values numerically extracted from the measurements performed at different voltages and angles.

### B. Numerical calculations of TMR curves with uniaxial anisotropy

A numerical calculation of TMR($H$) curves within the hypothesis of a uniaxial anisotropy along **n** was performed. The details of the calculation are given in the Appendix, where we suppose that the energy of an individual cluster is given by $E = -\mu_0 \mathbf{H} \cdot \mathbf{m} + k_u \sin^2(\mathbf{n},\mathbf{m})$, where $k_u$ is the value of the uniaxial anisotropy along **n** for an individual cluster and $(\mathbf{n},\mathbf{m})$ is the angle between **n** and **m**. At a given temperature and magnetic field **H**, and for a given $k_u$ value, we calculate the partition function of the magnetic dipoles as in Ref. [22] and we extract the exact average value of $\cos(\mathbf{M}_1,\mathbf{m})$—or $\cos(\mathbf{M}_2,\mathbf{m})$— from which the TMR($H$) value is readily deduced.

First, if we focus on the numerical results obtained at an angle $\theta = 0$, we observe that the curves can still be fitted by Langevin curves, even when $k_u \neq 0$ (see Fig. 4). The magnetic anisotropy implies that the required $m$ value in the Langevin fits, defined as $m_{\text{eff}}$, appears larger than if $k_u$ were actually zero. This thus confirms that we cannot discriminate between an isotropic or anisotropic magnetic configuration through TMR measurements at $\theta = 0$.

We then turn to curves calculated for $\theta \neq 0$ to which we fitted experimental TMR($H$) curves. Here we have to find
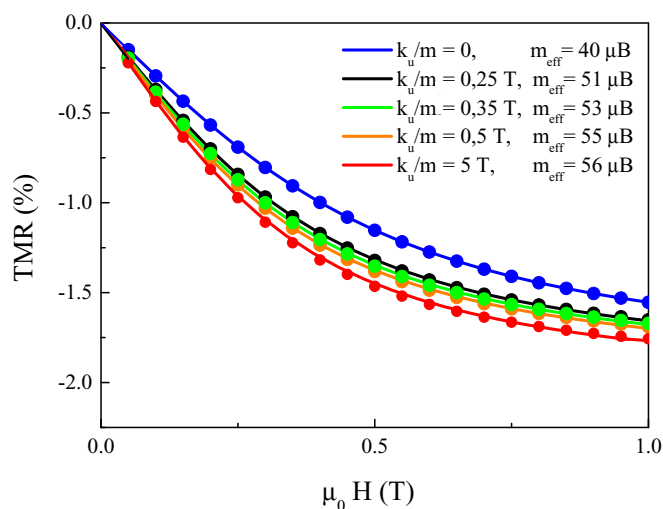


FIG. 4. (Color online) TMR($H$) values from the numerical simulation, calculated at $\theta = 0$ with $m = 40\mu_B$, with varying magnetic anisotropy value $k_u$ from zero to $2k_u/m = 10$ T (scatter dots). Fit by Langevin functions of the calculated curves (lines). The values of $m_{\text{eff}}$ extracted from these fits is given in the figure.
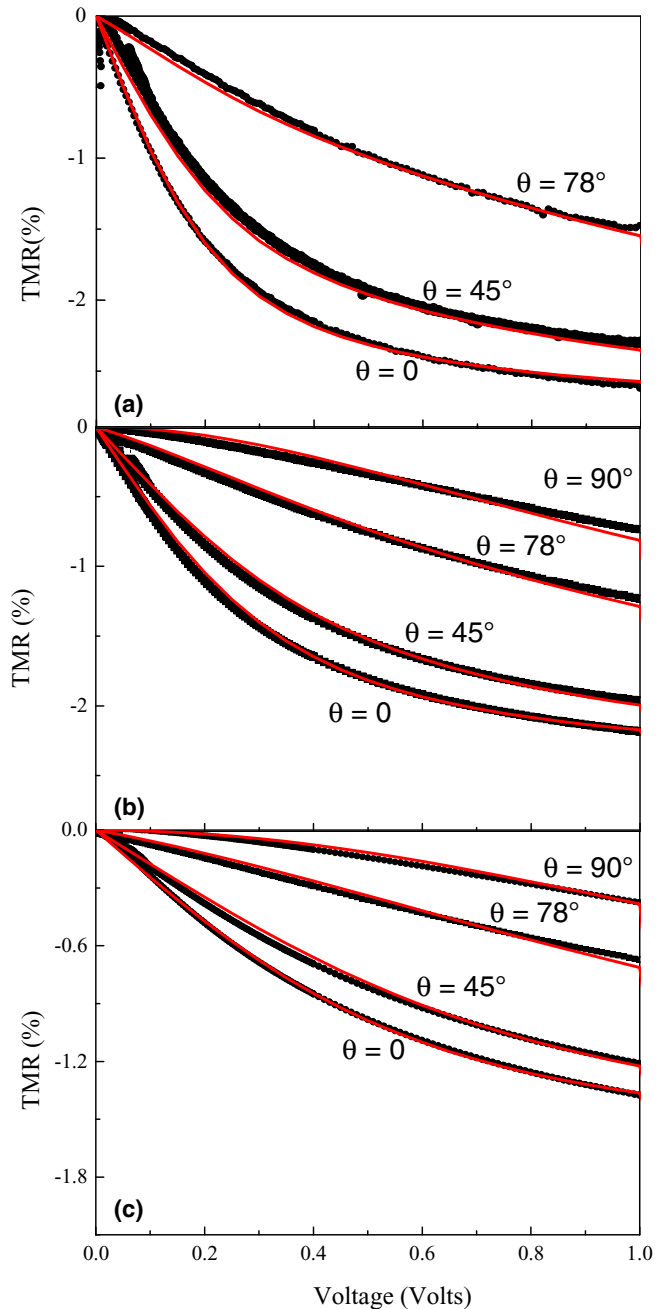


FIG. 5. (Color online) Measured TMR($H$) curves, at different angles $\theta$ and voltage values $V$, with fits from the numerical simulation, taking into account a nonzero magnetic anisotropy value $k_u$. The fits were performed simultaneously for a given voltage. (a) $V = -50$ mV. (b) $V = -200$ mV. (c) $V = -600$ mV.

the two parameters $k_u$ and $m$ that enable us to reproduce all the experimental TMR curves for the different measurement angles $\theta$ at a given voltage.

We show on Fig. 5 that we can indeed well fit the series of experimental curves, even at a given high voltage, by supposing a single $k_u$ value for all angles; for instance for $k_u = 0.78$ meV at $-200$ mV and for $k_u = 1.16$ meV at $-600$ mV. This clearly suggests the presence of a uniaxial anisotropy that increases with the applied electric field.
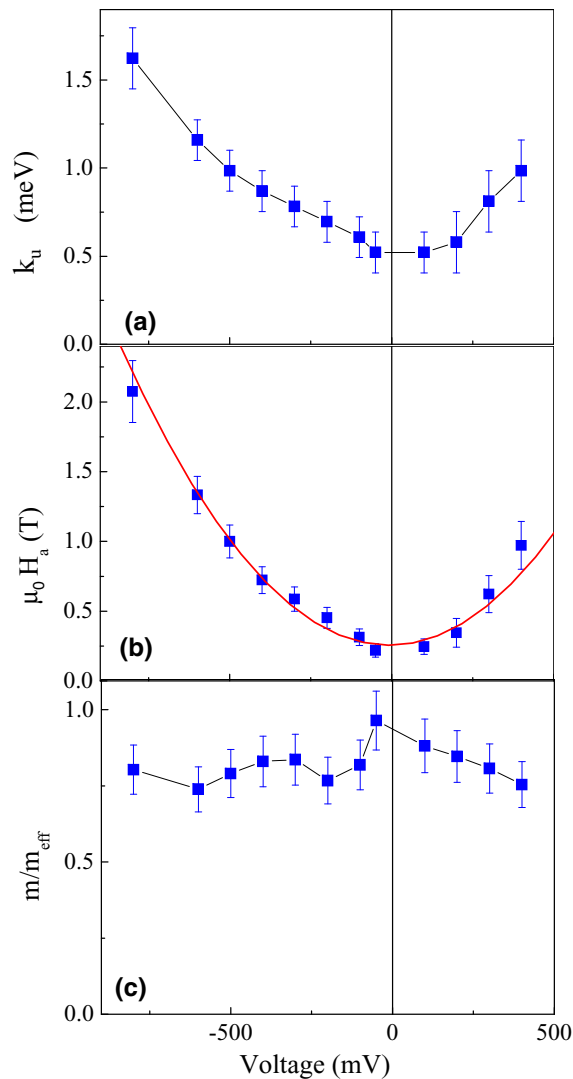
FIG. 6. (Color online) (a) $k_u$ values from fits of the experimental data with numerical simulations. (b) $\mu_0 H_a = 2k_u/m$ as a function of the applied voltage. The red line is a parabolic fit of experimental data. (c) Ratio of $m$ to $m_{\mathrm{eff}}$ obtained respectively through fits supposing $k_u \neq 0$ and $k_u = 0$ for curves measured at $\theta = 0$.

### C. Voltage-driven magnetic anisotropy

The evolution of the value of $k_u$ with the applied voltage, obtained from fits similar to the ones shown on Fig. 5, is given on Fig. 6(a): $k_u(V)$ is an almost even and increasing function of the voltage. At zero bias, we can extrapolate that there is a non-negligible magnetic anisotropy [$k_u(0) = 0.52$ meV]. The anisotropy value, in the meV range, compares with the thermal fluctuation energy $k_B T$ of close to 0.5 meV at 6 K. The anisotropy is thus not large enough to force the cluster magnetization to remain confined in the plane, but has a strong influence on its orientation. This effect can be more intuitively described through an evaluation of the anisotropy field, defined as $\mu_0 H_a = 2k_u/m$. $H_a$ varies approximately quadratically with $V$, as shown on Fig. 6(b). This magnetic field can be extrapolated to about 0.23 T at zero voltage and reaches 2 T at $-800$ mV [Fig. 6(a)]; we thus observe a 1000% change of the anisotropy field by applying less than 1 V to the

junctions. This effect is related to a concomitant decrease of $m$ and an increase of $k_u$ upon increasing the applied voltage. The origin of this large electric-field-induced anisotropy field relies either on the large strain in the clusters, which could lead to an intrinsic modification of the $Cr_2O_3$ magnetoelectric properties, or on magnetic anisotropy at the $MgO/Cr_2O_3$ and $Cr_2O_3/MgO$ interfaces due to electric charge accumulation under bias voltage. Within the first hypothesis, **n** would appear as a strong hard axis because of the biaxial in-plane compressive strain in the epitaxial clusters: we indeed found in Ref. [9] that $Cr_2O_3$ clusters are epitaxial on MgO[100], with their [11$\bar{1}$0] direction along the normal to the layer [Fig. 1(a)]. This direction, contrary to the $c$-axis direction [23,24], is not expected to be a high-anisotropy axis, as it is a sixfold-symmetry axis within the corundum structure. In our case we could suppose that the high epitaxial compressive strain [9] of $Cr_2O_3$ on MgO breaks the symmetry in the $Cr_2O_3(001)$ plane and induces this voltage-driven perpendicular magnetic anisotropy along **n**; the biaxial strain could thus enhance the magnetoelectric effect along the normal direction. Such an electric-field-induced magnetic anisotropy was for instance predicted by Hu *et al.* in Ref. [25] along the normal to planar phtalocyanine molecules.

On the other hand, there are a number of studies proving that the magnetic anisotropy at the interface with oxides, especially in MgO-based magnetic tunnel junctions [12,15,26], is sensitive to the applied electric field. It was clearly attributed [27,28] to a voltage-induced change of the metal $d$-band occupancy, resulting from the hybridization of metal electronic states with oxygen at the interface with the insulating oxide. We also can draw a parallel between our observations and the work recently reported by Sonntag *et al.* [29] on 4-nm-diameter Fe nanomagnets observed by scanning tunneling microscopy, in the absence of interfaces with oxides. They showed a voltage-induced linear change in the Fe cluster anisotropy $\Delta k_u$, reaching up to 2 meV per cluster under a 6 GV/m electric field, which corresponds to a 6% change in the absolute anisotropy energy value. They also attributed this effect to electron accumulation at the cluster surface.

In our case, the surface charge density at the cluster interfaces, given by $\sigma = \varepsilon_0 \varepsilon_r E$, where $\varepsilon_r = 10$ for MgO and $E$ is the electric field through the MgO tunnel barrier, is close to $\sigma = 8$mC/m$^2$ at $-500$ mV, which is the charge density reached at $E = 1$ GV/m in the measurements of Sonntag *et al.* For this $\sigma$ value, they obtain a surface anisotropy change of 1.6 $\mu$J/m$^2$, and other values reported in the literature [12,15,26] range between 3.4 and 9.5 $\mu$J/m$^2$. We obtain 2.8 $\mu$J/m$^2$ in our case [Fig. 6(a)], at $-500$ mV, which is comparable with those values. As regards the voltage-induced anisotropy field change of $2\Delta k_u/m$, the observed value is much larger than in the case reported by Sonntag *et al.* [Fig. 6(b)]. This might be attributed to the low magnetization (in the $0.01\mu_B$ range per $Cr^{3+}$ atom) in our $Cr_2O_3$ weak ferromagnetic clusters [9].

The voltage-induced anisotropy energy values that we obtain could thus support the scenario of an interfacial effect, but we have to keep in mind that the studied systems are not the usual Fe or Co layers at oxide interfaces but a weak ferromagnetic $Cr_2O_3$ oxide [9]. There is *a priori* no reason why we should obtain the same $\Delta k_u$ values as in the literature. Moreover, the anisotropy changes reported in past

years [26,29] are mostly linear in the electric field, with a sign change at zero voltage. In our case the anisotropy field curve is even, and follows a more quadratic behavior [Fig. 6(b)], but we are dealing with symmetric stacks, involving two interfaces, not one, in contrast to the above-mentioned works. Calculations performed on symmetric MgO/Fe/MgO stacks by Shimabukuro *et al.* [28] also predict an even and nonlinear change of $\Delta k_u$ with the applied bias voltage. The scenario of a magnetic anisotropy change localized at the interface due to charge accumulation is thus probable, but cannot be asserted.

Another more speculative mechanism, which would rely on a coupling between superparamagnetism and superparaelectricity in the clusters' assembly, cannot be ruled out. We indeed showed in Ref. [9] that the $Cr_2O_3$ nanoparticles carried a very weak electric dipole. Applying an electric field along **n** aligns those electric dipoles and could influence the magnetic moment direction if the two moments, electric and magnetic, were coupled.

Finally, taking into account the observed strong magnetic anisotropy, we should make a correction in our previous evaluations of the variation of $m$ with the electric field. We indeed showed that $m$, the typical cluster magnetic moment, decreased with the electric field; its value was calculated supposing that the cluster magnetization remained isotropic for all voltages—corresponding thus to $m_{eff}$ [9]. This is actually not the case, as magnetic moments are more confined in plane at high voltages. Figure 6(c) shows that the relative discrepancy due to this assumption increases with the $k_u$ value, and thus with the absolute applied voltage, but remains moderate, lower than 30% even at −800 mV. It moreover shows that we overestimated in our previous article the $m_{eff}$ value at high voltages, whereas the low-voltage value was correct. We therefore underestimated the magnetoelectric effect on the magnetization modulus of about 30% between 0 and 1 V in Ref. [9].

## IV. CONCLUSION

An assembly of $Cr_2O_3$ nanoparticles embedded in a MgO matrix exhibits a change of the magnetization direction under an electric field, with a preferred magnetization direction transverse to the applied electric field. This effect is observed for electric fields in the GV/m range, and corresponds to an increase of the magnetic anisotropy field of one order of magnitude, under 1 V. We also show that this effect, although large, does not preclude our previous estimations of a large change of the individual magnetization modulus of the clusters under an applied voltage [9].

The question of the microscopic origin of the electric-field-induced magnetic anisotropy remains open: this is due either to a strain-induced enhancement of the magnetoelectric coefficient in those epitaxial clusters or to a charge accumulation at the $Cr_2O_3$/MgO interfaces under bias voltage. The anisotropy energy changes observed under an applied electric field compare well with values reported in different systems at the interface between an oxide and a ferromagnetic layer. This would support the second hypothesis, but further studies, with an electric field applied in plane, should allow discrimination between the two main hypotheses.

## APPENDIX: CALCULATION OF THE TMR($H$) CURVES WITHIN THE HYPOTHESIS OF A UNIAXIAL ANISOTROPY $k_u$

We here give the detailed calculation of the total magnetization of clusters within the hypothesis of a uniaxial anisotropy along the normal to the plane, **n**. This calculation is also used to evaluate the TMR in the isotropic case, by supposing no uniaxial anisotropy in the energy formula.

For simplicity's sake, we suppose that the in-plane components of $\mathbf{M}_1$ and $\mathbf{M}_2$ are parallel, not antiparallel. This is true, provided **H** is above the coercive field of both electrodes. Both Fe and Fe/Co electrodes have an easy in-plane magnetization. The out-of plane component of the magnetic field $\mathbf{H}_z$ will therefore force their magnetizations $\mathbf{M}_1$ and $\mathbf{M}_2$ out of this easy plane. Taking into account the shape magnetic anisotropy in the electrodes, the out-of-plane component of their magnetization is linear in $\mathbf{H}_z$, given by $\tan(\theta_0) = \mu_0 H \sin(\theta)/H_d$, where $\mu_0 H_d = 2.2$ T in the case of our Fe electrodes. We also suppose that $H_{d1} = H_{d2} = H_d$. $\mathbf{M}_1$ and $\mathbf{M}_2$ thus make the same angle $\theta_0$ relative to the plane.

If we now calculate the resistance of the junction—regarded as two tunnel junctions in series—in this magnetic configuration, for one given cluster of magnetic moment **m**, we get

$$R(H) = R_1 + R_2 + \Delta R_1 \cos(\mathbf{m},\mathbf{M}_1) + \Delta R_2 \cos(\mathbf{m},\mathbf{M}_2),$$

where (**a**,**b**) is the angle between the **a** and **b** directions, $R_1$ and $R_2$ are the spin-independent resistances of the two tunnel junctions, and $\Delta R_1$ and $\Delta R_2$ the spin dependent parts [20]. The average value for $R$ is, as the direction of **m** fluctuates, obtained through the average value of $\cos(\mathbf{m},\mathbf{M}_1)$ and $\cos(\mathbf{m},\mathbf{M}_2)$ which are supposed to be equal.
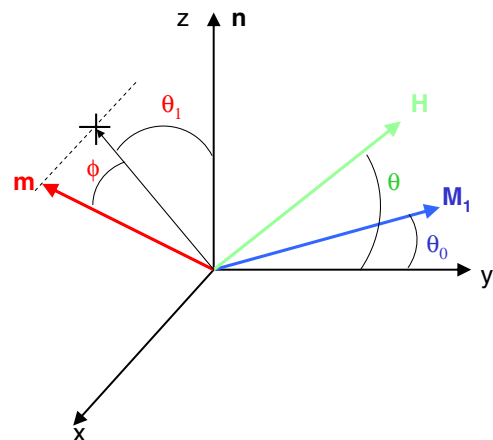


FIG. 7. (Color online) Scheme of the angles used in the calculation shown in the Appendix. $(x,y)$ is the plane of the thin films. **H** and $\mathbf{M}_1$ are in the $(y,z)$ plane. **n** is taken along $z$. **m** is *a priori* free to rotate in all directions.

The magnetic energy of one cluster is given by

$$E = -\mu_0 H m + k_u M_z^2 = -\mu_0 H m \times [\sin\theta\cos\phi\cos\theta_1 \\ + \cos\theta\cos\phi\sin\theta_1] + k_u[\cos\phi\cos\theta_1],$$

[2] where the angles are defined on Fig. 7.

In order to calculate the TMR values, we calculate the average value of $\cos(\mathbf{m}, \mathbf{M}_1) = \cos\theta_0\cos\phi\sin\theta_1 + \sin\theta_0\cos\phi\cos\theta_1$,

which can be written

$$\langle\cos(\mathbf{m}, \mathbf{M}_1)\rangle = \frac{1}{Z}\int_{\theta_1=0}^{2\pi}\int_{\phi=-\pi/2}^{\pi/2}\cos\phi\cos(m, M_1) \\ \times e^{-E/k_B T}d\theta_1 d\phi,$$

where the partition function $Z$ is written $\int_{\theta_1=0}^{2\pi}\int_{\phi=-\pi/2}^{\pi/2}\cos(\phi)e^{-E/k_B T}d\theta_1 d\phi$ and $\theta_0$ is defined by $\mathrm{atan}(\theta_0) = \mu_0 H\sin\theta/H_d$.

TheTMR($H$) curves are readily deduced from this calculation.

---

[1] D. N. Astrov, Sov. Phys. JETP **11**, 708 (1960).

[2] X. He, Y. Wang, N. Wu, A. N. Caruso *et al.*, Nat. Mater. **9**, 579 (2010).

[3] S. Sahoo and C. Binek. Philos. Mag. Lett. **87**, 259 (2007).

[4] C. J. Fennie and K. M. Rabe, Phys. Rev. Lett. **97**, 267602 (2006).

[5] M. D. Glinchuk, E. A. Eliseev, A. N. Morozovska, and R. Blinc, Phys. Rev. B **77**, 024106 (2008).

[6] A. N. Morozovska, M. D. Glinchuk, and E. A. Eliseev, Phys. Rev. B **76**, 014102 (2007).

[7] M. D. Glinchuk, E. A. Eliseev, and A. N. Morozovska, Phys. Rev. B **78**, 134107 (2008).

[8] C. G. Duan, C. W. Nan, S. S. Jaswal, and E. Y. Tsymbal, Phys. Rev. B **79**, 140403 (2009).

[9] D.Halley, N. Najjari, H. Majjad, L. Joly *et al.*, Nat. Commun. **5**, 3167 (2014).

[10] Z. Wang, Y. Yang, R. Viswan, J. Li, and D. Viehland, Appl. Phys. Lett. **99**, 043110 (2011).

[11] M. Weisheit, S. Fähler, A. Marty, Y. Souche, C. Poinsignon, and D. Givord, Science **315**, 349 (2007).

[12] T. Maruyama, Y. Shiota, T. Nozaki, K. Ohta *et al.*, Nat. Nano **4**, 158 (2009).

[13] W. G. Wang, M. Li, S. Hageman, and C. L. Chien, Nat. Mater. **11**, 65 (2012).

[14] O. Fruchart, P. O. Jubert, C. Meyer, M. Klaua, J. Barthel, and J. Kirschner, J. Magn. Magn. Mater. **239**, 224 (2002).

[15] T. Nozakki, Y. Shiota, M. Shiraishi, T. Shinjo, and Y. Suzuki, Appl. Phys. Lett. **96**, 022506 (2010).

[16] D. Halley, M. Bowen, H. Majjad, N. Najjari *et al.*, Appl. Phys. Lett. **92**, 212115 (2008).

[17] S. Yuasa, T. Nagahama, A. Fukushima, Y. Susuki, and K. Ando, Nat. Mater. **3**, 868 (2004).

[18] T. Koda, S. Mitani, M. Mizogushi, and K. Takanashi, J. Phys.: Conf. Ser. **266**, 012093 (2011).

[19] R. Matsumoto *et al.*, Phys. Rev. B **79**, 174436 (2009).

[20] S. Maekawa, S. Takahashi and H. Imamura, in *Spin Dependent Transport in Magnetic Nanostructures*, edited by S. Maekawa and T. Shinjo (CRC Press, Boca Raton, FL, 2002), Chap. 4.

[21] W. H. Butler, X.-G. Zhang, T. C. Schulthess, and J. M. MacLaren, Phys. Rev. B **63**, 092402 (2001).

[22] F. Wiekhorst, E. Shevchenko, H. Weller, and J. Kötzler, Phys. Rev. B **67**, 224416 (2003).

[23] J. O. Artman, J. C. Murphy, and S. Foner, J. Appl. Phys. **36**, 986 (1965).

[24] M. Fiebig, D. Fröhlich, and H. J. Thiele, Phys. Rev. B **54**, R12681(R) (1996).

[25] J. Hu and R. Wu, Phys. Rev. Lett. **110**, 097202 (2013).

[26] M. Endo, S. Kanai, S. Ikeda, F. Matsukura, and H. Ohno, Appl. Phys. Lett. **96**, 212503 (2010).

[27] K. Nakamura, T. Akiyama, T. Ito, M. Weinert, and A. J. Freeman, Phys. Rev. B **81**, 220409(R) (2010).

[28] R. Shimabukuro, K.Nakamura, T. Akiyama, and T. Ito, Physica E **42**, 1014 (2010).

[29] A. Sonntag, J. Hermenau, A. Schlenhoff, J. Friedlein, S. Krause and R. Wiesendanger, Phys. Rev. Lett. **112**, 017204 (2014).